

ORIGINAL RESEARCH



Spatial immune heterogeneity of hypoxia-induced exhausted features in high-grade glioma

A-Reum Kim^{a,*,#}, Seong Jin Choi^a, Junsik Park^a, Minsuk Kwon^a, Tamrin Chowdhury^b, Hyeon Jong Yu^b, Sojin Kim^b, Ho Kang^b, Kyung-Min Kim^b, Su-Hyung Park^a, Chul-Keek Park^b, and Eui-Cheol Shin^{a,c,*,#}

^aGraduate School of Medical Science and Engineering, Korea Advanced Institute of Science and Technology (KAIST), Daejeon, Republic of Korea; ^bDepartment of Neurosurgery, Seoul National University College of Medicine, Seoul National University Hospital, Seoul, Republic of Korea; ^cThe Center for Epidemic Preparedness, KAIST Institute, Daejeon, Republic of Korea

ABSTRACT

The tumor immune microenvironment (TIME) in high-grade glioma (HGG) exhibits high spatial heterogeneity. Though the tumor core and peripheral regions have different biological features, the cause of this spatial heterogeneity has not been clearly elucidated. Here, we examined the spatial heterogeneity of HGG using core and peripheral regions obtained separately from the patients with HGG. We analyzed infiltrating immune cells by flow cytometry from 34 patients with HGG and the transcriptomes by RNA-seq analysis from 18 patients with HGG. Peripheral region-infiltrating immune cells were *in vitro* cultured in hypoxic conditions and their immunophenotypes analyzed. We analyzed whether the frequencies of exhausted CD8⁺ T cells and immunosuppressive cells in the core or peripheral regions are associated with the survival of patients with HGG. We found that terminally exhausted CD8⁺ T cells and immunosuppressive cells, including regulatory T (T_{REG}) cells and M2 tumor-associated macrophages (TAMs), are more enriched in the core regions than the peripheral regions. Terminally exhausted and immunosuppressive profiles in the core region significantly correlated with the hypoxia signature, which was enriched in the core region. Importantly, *in vitro* culture of peripheral region-infiltrating immune cells in hypoxic conditions resulted in an increase in terminally exhausted CD8⁺ T cells, CTLA-4⁺ T_{REG} cells, and M2 TAMs. Finally, we found that a high frequency of PD-1⁺CTLA-4⁺CD8⁺ T cells in the core regions was significantly associated with decreased progression-free survival of patients with HGG. The hypoxic condition in the core region of HGG directly induces an immunosuppressive TIME, which is associated with patient survival.

ARTICLE HISTORY

Received 12 August 2021
Revised 3 January 2022
Accepted 3 January 2022

KEYWORDS

High-grade glioma; immune cell; T cell; tumor microenvironment; hypoxia



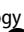
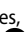
Introduction

High-grade glioma (HGG) is an aggressive central nervous system (CNS) tumor, comprising World Health Organization (WHO) grade 3 (e.g., anaplastic astrocytoma and anaplastic oligodendroglioma) and grade 4 (e.g., glioblastoma) tumors,¹ and representing 24.1% of primary brain tumors.² Despite a standard treatment regimen, prognosis remains poor because of high heterogeneity of inter/intra-tumor and the complex mechanism underlying HGG tumorigenesis.³

The CNS has traditionally been considered an immunologically privileged site because it is sequestered by the blood-brain barrier (BBB). However, a lymphatic system was recently discovered in the CNS, indicating that it is an immunologically active site.⁴ Moreover, the BBB is compromised in brain tumors and, as in other tumors, diverse immune cells infiltrate the brain tumor tissue.⁵ Brain tumor-infiltrating immune cells include not only anti-tumor effector cells, but also various anti-inflammatory cells that contribute to the immunosuppressive brain tumor-immune


microenvironment (TIME).^{6,7} Therefore, tumor-infiltrating immune cells are an attractive target for modulating the TIME for HGG therapy.

In tumor tissues, CD8⁺ T cells are a part of the immune infiltrate and key effectors with anti-tumor functions. However, upon chronic persistent stimulation by tumor antigen, CD8⁺ T cells differentiate into a dysfunctional or exhausted state.^{8,9} Exhausted CD8⁺ T cells are characterized by high expression of immune checkpoint inhibitory receptors, including programmed cell death protein 1 (PD-1), cytotoxic T-lymphocyte antigen 4 (CTLA-4), T-cell immunoglobulin and mucin-domaincontaining-3 (TIM-3), and T-cell immunoglobulin and immunoreceptor tyrosine-based inhibitory motif domain (TIGIT).¹⁰⁻¹⁴ Moreover, several transcriptional factors/DNA-binding factors are known to regulate the exhaustion and differentiation of CD8⁺ T cells, including Eomes, T-bet, TCF-1, and TOX.¹⁵⁻¹⁹ In HGG, previous studies have

CONTACT Eui-Cheol Shin  ecshin0@gmail.com  Laboratory of Immunology and Infectious Diseases, Graduate School of Medical Science and Engineering, KAIST, 291 Daehak-ro, Yuseong-gu, Daejeon 34141, Republic of Korea; Chul-Keek Park  nsckpark@snu.ac.kr  Department of Neurosurgery, Seoul National University College of Medicine, Seoul National University Hospital, 101 Daehak-ro, Jongno-gu, Seoul 03080, Republic of Korea

*These authors contributed equally to this work.

#Current address: The Center for Viral Immunology, Korea Virus Research Institute, Institute for Basic Science, Daejeon 34141, Republic of Korea

 Supplemental data for this article can be accessed on the [publisher's website](#)

© 2022 The Author(s). Published with license by Taylor & Francis Group, LLC.

This is an Open Access article distributed under the terms of the Creative Commons Attribution-NonCommercial License (<http://creativecommons.org/licenses/by-nc/4.0/>), which permits unrestricted non-commercial use, distribution, and reproduction in any medium, provided the original work is properly cited.

shown increased expression of immune checkpoint inhibitory receptors on tumor-infiltrating CD8⁺ T cells^{20,21} and terminally exhausted features.²²

In addition to CD8⁺ T cells, regulatory T (T_{REG}) cells infiltrate tumors and suppress anti-tumor immune responses.²³ T_{REG} cells in tumors exhibit a highly activated phenotype with strong expression of PD-1, CTLA-4, OX40, and other molecules.^{24,25} Various tumors also contain tumor-associated macrophages (TAMs), which express immunosuppressive cytokines and reduce the anti-tumor activity.^{26,27} In particular, TAMs differentiate into polarized M2 cells when exposed to tumor-derived IL-4, M-CSF, transforming growth factor (TGF)- β , or other molecules.^{28,29} Several studies have demonstrated the infiltration of T_{REG} cells and M2-type TAMs in HGG.^{30–34}

The tumor core and peripheral regions have already been shown to have different biological features. In general, core regions are more hypoxic and acidic than peripheral regions.^{35–37} In addition, core regions have more T_{REG} cells, myeloid-derived suppressor cells, and TAMs than peripheral regions,^{38,39} indicating that the microenvironment in core regions is more immunosuppressive than that in the peripheral regions. This is in line with the tumor core and peripheral regions having different microenvironments in HGG.^{40–42} In single-cell transcriptomic analysis of HGG tissues, core regions demonstrated more myeloid cells with hypoxic features.⁴¹ In addition, an immunohistochemistry study of HGG revealed that core regions have more exhausted and suppressive immune cells than peripheral regions.⁴² However, previous studies did not determine why core regions have more exhausted and suppressive immune cells in HGG. In addition, the clinical relevance of T-cell exhaustion and suppressive immune cells in the core/peripheral regions remains to be elucidated.

In the present study, we examined differences in the composition and phenotypes of tumor-infiltrating immune cells between the core and peripheral regions of HGG using multi-color flow cytometric analysis. We also examined transcriptional differences between the core and peripheral regions using RNA-seq analysis. We show that the core regions have more exhausted CD8⁺ T cells and immunosuppressive cells and demonstrate that the hypoxic condition directly increases CD8⁺ T-cell exhaustion and immunosuppressive cells in an *in vitro* culture system. Finally, we show that the relative frequency of severely exhausted CD8⁺ T cells in core regions is significantly associated with patient survival.

Materials and methods

Patient characteristics

Thirty four patients with HGG were enrolled in this study. The patients had homogeneously undergone current best clinical practice including maximal safe resection (complete resection in all cases) and adjuvant radiotherapy and chemotherapy depending on their WHO grades. Informed consent was obtained from all patients included in this study in accordance with the institutional review board at Seoul National University Hospital (IRB approval no. H-1902-

062-1010). The clinicopathological characteristics of the patients are presented in Table S1. The patients whose samples were used in this study did not receive any prior treatment other than routine short-course steroids and anti-epileptic drugs. Intravenous dexamethasone (4 mg) was uniformly administered to all patients four times in the 24 hours prior to surgery to enhance the intraoperative fluorescence of the tumor tissue.

Tissue collection

Fresh tumor tissues were obtained from 34 patients undergoing surgical resection of HGG after oral administration of 5-aminolevulinic acid (5-ALA, Gliolan[®]; Medac, Wedel, Germany).^{43,44} Histological diagnosis consisted of 26 glioblastomas (GBMs), 4 anaplastic oligodendrogliomas (AOs), and 4 anaplastic astrocytomas (AAs). Tissue specimens were collected separately from the core and peripheral areas of tumor tissue showing positive and negative fluorescence, respectively, and immersed in RPMI media at room temperature immediately after surgical resection. The MACS brain tumor dissociation kit (Miltenyi Biotec, Auburn, CA, USA) and gentleMACS[™] Dissociators (Miltenyi Biotec) were used to dissociate the tissue samples within 2 hours after collection, and debris was removed using MACS Debris Removal Solution (Miltenyi Biotec) according to the manufacturer's protocol. Only the samples with cell viability > 80% after dissociation were used in this study. Isolated single cells were cryopreserved until further use.

Flow cytometry

Cryopreserved single cell suspensions were thawed and stained using the LIVE/DEAD Fixable Aqua Dead Cell Stain Kit (Invitrogen, Carlsbad, CA, USA). The cells were then washed once and stained with fluorochrome-conjugated antibodies in the dark at 4°C for 20 minutes. For intracellular staining, the cells were fixed and permeabilized using the Foxp3 staining buffer kit (eBioscience) following the manufacturer's instructions. Multicolor flow cytometry was performed using an LSR II flow cytometer (BD Bioscience, NJ, USA) and the data analyzed by FlowJo V10 software (Treestar, San Carlos, CA, USA). The antibodies used for flow cytometry are listed in Table S2.

Cell quantification analysis

The number of isolated live single cells from tumor tissues was measured as the cell number/gram of tumor tissue. In flow cytometric analysis, the percentage of CD45⁺ cells among the total singlet cells was first determined. Each immune cell subset was identified by specific lineage markers. The gating strategy for each immune cell subset is presented in Figure S1. The percentage of each immune cell subset among the CD45⁺ cells was determined, and the number of cells in each immune cell subset was calculated as the cell number/gram of tumor tissue by multiplying the above values.⁴⁵

RNA sequencing

Total RNA was isolated from the core and peripheral areas of tumor tissue obtained from 18 GBM patients using the RNeasy Lipid Tissue Mini Kit (Qiagen, Maryland, USA). The compatible library was prepared using the TruSeq stranded total RNA LT sample prep kit (Illumina, San Diego, CA, USA) according to the manufacturer's instructions. Sequencing was achieved with the NovaSeq 6000 system (Illumina). Paired-end reads with 75 base pairs were aligned to the human reference genome using STAR (v 2.7.2).⁴⁶ Read counts were normalized for effective library size, and differentially expressed genes were analyzed using DESeq2.⁴⁷

In vitro hypoxic cultures of tumor-infiltrating immune cells

To validate hypoxic conditions, cryopreserved cells from the dissociated peripheral tumor were thawed, suspended in RPMI-1640 medium (WelGENE, Republic of Korea) containing 10% FBS (Corning, Arizona, USA) and 1% penicillin/streptomycin (WelGENE) without any cytokines and incubated in the presence of 0.5 μ M Image-iT Green Hypoxia Reagent (Invitrogen) for 6 hours under 21% or 1% oxygen using invivoO2 400 (RUSKINN BAKER, UK). To examine the effect of hypoxia on the immunophenotypes of tumor-infiltrating cells, thawed cells were suspended in the medium and incubated for 72 hours under 21% or 1% oxygen.

In addition, to examine the effect of hypoxia on the proliferation of CD8⁺ T cells from the peripheral region of HGG, thawed cells were labeled with CellTrace Violet (CTV; Invitrogen) according to the manufacturer's instructions. CTV-labeled cells were suspended in the medium and stimulated with 1 ng/ml plate-bound anti-CD3 (clone OKT3; eBioscience) for 96 hours under 21% or 1% oxygen. The proliferation of CD8⁺ T cells was analyzed by CTV dilution.

Statistics

Statistical analyses were performed using Prism 7 (GraphPad Software) and verified using R (v 4.1.0). The D'Agostino-Pearson normality test was used to examine the distribution of variables in each statistical analysis. We used the paired student's t-test and Wilcoxon matched-pairs signed rank test for parametric and non-parametric data, respectively. A Spearman correlation test was performed to assess the significance of the statistical correlation. Kaplan-Meier curves with the log-rank test were used to compare survival outcomes. Hazard ratios were calculated using multivariate Cox proportional hazard models. Significance was set at $P < .05$.

In RNA sequencing data analysis, differentially expressed genes were defined by an adjusted p -value $< .05$ and an absolute fold change > 2 . Gene set enrichment analysis was conducted with gene sets in the MSigDB Collection (h.all.v7.0.symbols.gmt) using the R package clusterProfiler (v 3.14).⁴⁸ The enrichment score for each sample was determined by single sample enrichment analysis with gene sets (h.all.v7.0.symbols.gmt; c5.bp.v7.0.symbols.gmt) in the R package GSEA (v 3.12).⁴⁹

Results

Immune cell compositions are different between the core and peripheral regions of HGG

In the present study, we obtained the core and peripheral regions of HGG (n = 34), prepared single-cell suspensions, and examined the immune cell composition by flow cytometry, including CD3⁺, CD4⁺, and CD8⁺ T cells, NK cells, B cells, monocytes, and dendritic cells (DCs) among CD45⁺ cells (Figure S1 and S2). The relative frequencies of CD3⁺ and CD4⁺ T cells and monocytes were significantly higher in the core region than in the peripheral region, whereas the relative frequencies of CD8⁺ T cells, NK cells, and B cells were not different between the core and peripheral regions ($P = .0008$ for CD3⁺ cells, $P < .0001$ for CD4⁺ cells, $P = .1012$ for CD8⁺ cells, $P = .1862$ for CD56⁺ cells, $P = .2491$ for CD19⁺ cells, $P < .0001$ for CD68⁺ cells, $P = .0087$ for CD163⁺ cells, $P < .0001$ for CD14⁺ cells; Figure 1a, Figure S3a). The relative frequency of DCs was higher in the peripheral region than in the core region ($P < .0001$). In addition, we analyzed the absolute numbers of immune cells. The number of CD45⁺ cells was significantly higher in the core region than in the peripheral region ($P < .0001$; Figure S3b). The numbers of CD3⁺, CD4⁺, and CD8⁺ T cells, NK cells, and monocytes were significantly higher in the core region than in the peripheral region, whereas the number of B cells was not different between the core and peripheral regions ($P < .0001$ for CD3⁺ cells, $P < .0001$ for CD4⁺ cells, $P < .0001$ for CD8⁺ cells, $P = .0005$ for CD56⁺ cells, $P = .2702$ for CD19⁺ cells, $P = .0003$ for CD68⁺ cells, $P = .003$ for CD163⁺ cells, $P = .0001$ for CD14⁺ cells; Figure S3c). The number of DCs was higher in the peripheral region than in the core region ($P = .0178$).

The expression levels of activation markers of CD11c⁺ cells, including CD80, CD86, and MHC class II (MHC-II), were also significantly higher in the peripheral region than in the core region ($P = .0156$ for CD80, $P = .0469$ for CD86, $P = .0469$ for MHC-II; Figure S4). These data indicate that the core and peripheral regions have different immune cell compositions.

CD8⁺ T cells in the core region exhibit a more severely exhausted phenotype

Although the relative frequency of CD8⁺ T cells did not differ between the core and peripheral regions, we focused on the phenotypic difference in CD8⁺ T cells between the two regions because CD8⁺ T-cell exhaustion is a hallmark in the TIME. First, we examined the expression of various immune checkpoint co-inhibitory receptors, including PD-1, CTLA-4, and TIM-3. The percentage of CTLA-4⁺ cells among CD8⁺ T cells was significantly higher in the core region than in the peripheral region ($P = .0023$), whereas the percentage of cells expressing the other receptors was not ($P = .0819$ for PD-1⁺ cells, $P = .5656$ for Tim-3⁺ cells; Figure 1b, Figure S5a). We examined the expression level of PD-1 on PD-1⁺CD8⁺ T cells and found that it was significantly higher in the core region than in the peripheral region ($P = .0273$; Figure 1c, Figure S5b). In addition, the percentage of PD-1⁺CTLA-4⁺ cells among CD8⁺ T cells was significantly higher in the core region than in the peripheral region ($P < .0001$; Figure 1d, Figure S5c). However, we found no difference in the expression of co-stimulating receptors, including TIGIT, 4-1BB, and OX40 ($P = .058$ for TIGIT⁺ cells, $P = .4037$ for 4-1BB⁺ cells, $P = .2312$

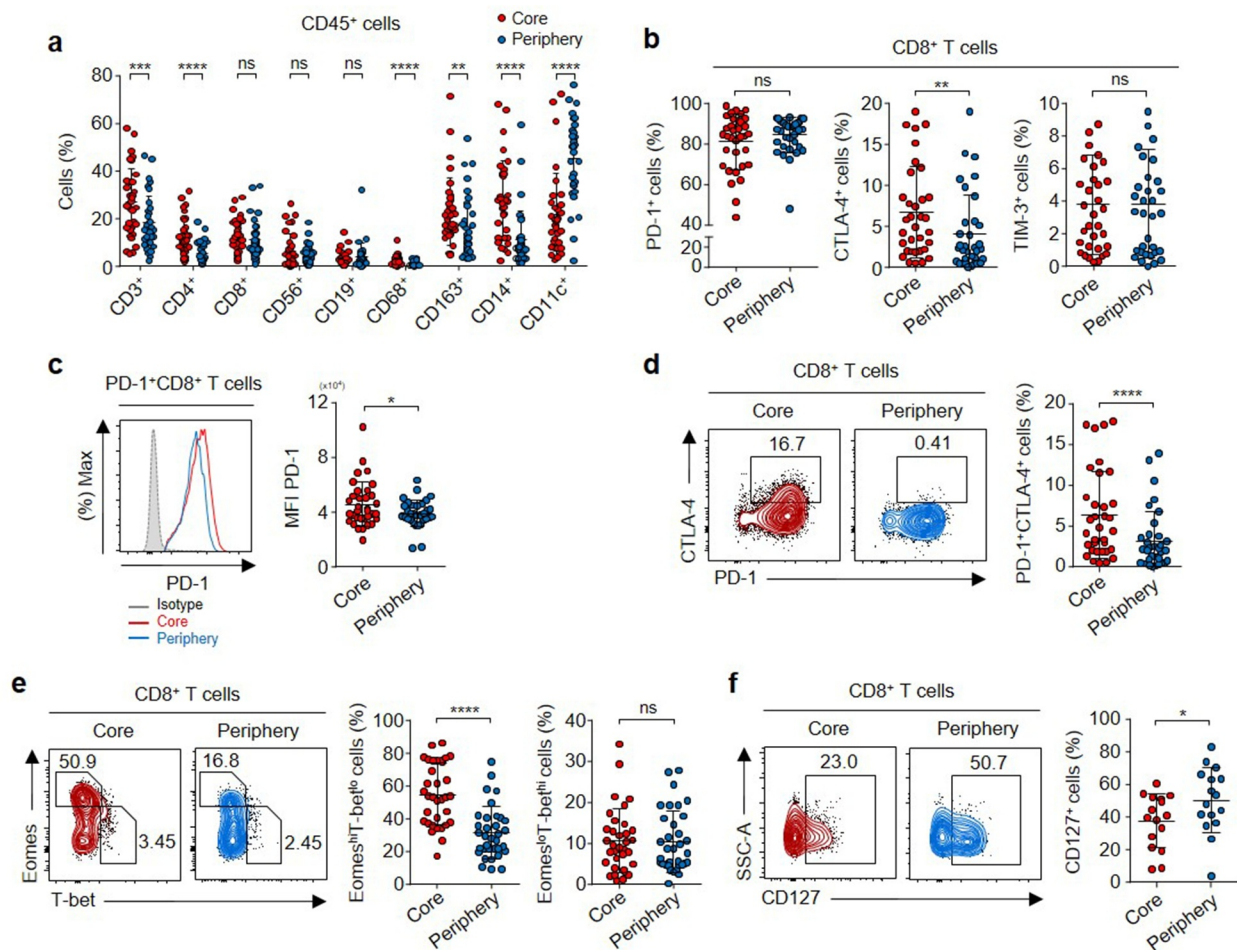


Figure 1. Immune cell composition and phenotypes of CD8⁺ T cells in the core and peripheral regions of HGG. Immune cell compositions (a) and paired tumor core and peripheral region-infiltrating CD8⁺ T cells (b-f) from HGG patients were analyzed by flow cytometry (n = 34). (a) The percentages of respective immune cells among CD45⁺ cells from the tumor core and peripheral regions. ns, not significant; ***P* < .01; ****P* < .001; *****P* < .0001; Wilcoxon matched-pairs signed rank test. (b) The percentages of PD-1⁺, CTLA-4⁺, and TIM-3⁺ (n = 34) cells among CD8⁺ T cells from paired tumor core and peripheral regions. ns, not significant; ***P* < .01; Wilcoxon matched-pairs signed rank test. (c) The expression level of PD-1 among PD-1⁺CD8⁺ T cells from paired tumor core and peripheral regions (n = 34). **P* < .05; Wilcoxon matched-pairs signed rank test. (d) The percentages of PD-1⁺CTLA-4⁺ cells among CD8⁺ T cells from paired tumor core and peripheral regions (n = 34). *****P* < .0001; Wilcoxon matched-pairs signed rank test. (e) Representative flow plot from a patient (no. 12). The percentages of Eomes^{hi}T-bet^{lo} cells and Eomes^{lo}T-bet^{hi} cells among CD8⁺ T cells from paired tumor core and peripheral regions (n = 34). ns, not significant; *****P* < .0001; Wilcoxon matched-pairs signed rank test. (f) Representative flow plot from a patient (no. 12). The percentages of CD127⁺ cells among CD8⁺ T cells from paired tumor core and peripheral regions (n = 16). **P* < .05; Wilcoxon matched-pairs signed rank test. All results were presented means ± SD (standard deviation).

for OX40⁺ cells; Figure S5d). The absolute numbers of CD8⁺ T cells expressing PD-1, CTLA-4, TIM-3, TIGIT, and 4-1BB were significantly higher in the core region than in the peripheral region (*P* < .0001 for PD-1⁺ cells, *P* < .0001 for CTLA-4⁺ cells, *P* = .0015 for TIM-3⁺ cells, *P* = .001 for TIGIT⁺ cells, *P* = .0042 for 4-1BB⁺ cells, *P* = .4037 for OX40⁺ cells; Figure S6a). In addition, the absolute number of PD-1⁺CTLA-4⁺CD8⁺ T cells was significantly higher in the core region than in the peripheral region (*P* < .0001; Figure S6b). These data suggest that CD8⁺ T cells in the core region are more severely exhausted than those in the peripheral region of HGG.

Next, to analyze the differentiation status of CD8⁺ T cells, we examined the expression of transcriptional factors related to T-cell differentiation. Eomes^{hi}T-bet^{lo}CD8⁺ T cells are terminally differentiated cells, whereas Eomes^{lo}T-bet^{hi}CD8⁺ T cells are progenitor-like cells among exhausted CD8⁺ T cells.^{15,50} We found that the percentage of Eomes^{hi}T-bet^{lo} cells among CD8⁺ T cells was significantly higher in the core region than in the peripheral region (*P* < .0001), whereas the percentage of Eomes^{lo}T-bet^{hi} cells was not

different (*P* = .6853; Figure 1e, Figure S5e). In addition, the percentage of cells expressing CD127, another marker of progenitor-like cells, among CD8⁺ T cells was significantly lower in the core region than in the peripheral region (*P* = .025; Figure 1f, Figure S5f). The absolute numbers of Eomes^{hi}T-bet^{lo}CD8⁺ T cells, Eomes^{lo}T-bet^{hi}CD8⁺ T cells, and CD127⁺CD8⁺ T cells were significantly higher in the core region than in the peripheral region (*P* < .0001 for Eomes^{hi}T-bet^{lo} cells, *P* = .0036 for Eomes^{lo}T-bet^{hi} cells, *P* = .0076 for CD127⁺ cells; Figure S6c, d). These data indicate that CD8⁺ T cells in the core region are more terminally exhausted than those in the peripheral region of HGG.

Immunosuppressive cells are more predominant in the core region

We also compared the relative frequency of immunosuppressive cells between the core and peripheral regions, including Foxp3⁺CD25⁺CD127^{lo}CD4⁺ T_{REG} cells and

CD163⁺CD68⁺CD14⁺ M2 TAMs. We found that the percentage of T_{REG} cells among CD45⁺ cells was significantly higher in the core region than in the peripheral region ($P < .0001$; Figure 2a, Figure S7a). We also analyzed T_{REG} subpopulations, including CD45RA⁺Foxp3^{lo} naïve T_{REG} cells and CD45RA⁻Foxp3^{hi} activated T_{REG} cells, which are known to exert stronger suppressive functions than naïve T_{REG} cells. We found that the percentage of activated T_{REG} cells was significantly higher in the core region than in the peripheral region ($P < .0001$; Figure 2b, Figure S7b). The percentage of naïve T_{REG} cells was close to 0 in both the core and peripheral regions. The absolute numbers of T_{REG} cells, naïve T_{REG} cells, and activated T_{REG} cells were significantly higher in the core region than in the peripheral region ($P < .0001$ for T_{REG} cells, $P < .0001$ for naïve T_{REG} cells, $P < .0001$ for activated T_{REG} cells; Figure S8a, b).

Next, we analyzed phenotype markers that are known to be upregulated in T_{REG} cells, including PD-1, CTLA-4, TIGIT, 4-1BB, and OX40. The percentages of cells expressing these markers among T_{REG} cells were significantly higher in the core region than in the peripheral region ($P < .0001$ for PD-1⁺ cells, $P = .0016$ for CTLA-4⁺ cells, $P < .0001$ for TIGIT⁺ cells, $P = .0034$ for 4-1BB⁺ cells, $P < .0001$ for OX40⁺ cells; Figure 2c, Figure S7c). Notably, CTLA-4 is directly involved in the suppressive function of T_{REG} cells.^{51,52} The absolute numbers of T_{REG} cells expressing these markers were also significantly higher in the core region than in the peripheral region

($P < .0001$ for PD-1⁺ cells, $P < .0001$ for CTLA-4⁺ cells, $P < .0001$ for TIGIT⁺ cells, $P < .0001$ for 4-1BB⁺ cells, $P < .0001$ for OX40⁺ cells; Figure S8c).

We also found that the percentage of non-T_{REG} cells (Foxp3⁻CD25⁻CD4⁺ cells) among CD45⁺ cells was significantly higher in the core region than in the peripheral region ($P < .0001$; Figure S9a). In addition, the percentages of cells expressing PD-1, CTLA-4, TIGIT, and 4-1BB among non-T_{REG} cells were significantly higher in the core region than in the peripheral region ($P = .0003$ for PD-1⁺ cells, $P = .0061$ for CTLA-4⁺ cells, $P < .0001$ for TIGIT⁺ cells, $P = .0226$ for 4-1BB⁺ cells, $P = .8774$ for OX40⁺ cells; Figure S9b). The absolute numbers of non-T_{REG} cells and non-T_{REG} cells expressing PD-1, CTLA-4, TIGIT, 4-1BB, and OX40 were significantly higher in the core region than in the peripheral region ($P < .0001$ for PD-1⁺ cells, $P < .0001$ for CTLA-4⁺ cells, $P < .0001$ for TIGIT⁺ cells, $P = .0002$ for 4-1BB⁺ cells, $P < .0001$ for OX40⁺ cells; Figure S10).

Moreover, we found that the percentages of CD163⁺CD14⁺ cells (M2 monocytes), CD68⁺CD14⁺ cells (TAMs), and CD163⁺CD68⁺CD14⁺ cells (M2 TAMs) among CD45⁺ cells were significantly higher in the core region than in the peripheral region ($P < .0001$ for all; Figure 3a, Figure S11a). Among CD14⁺ cells, we found that the percentages of CD68⁺ cells and CD163⁺CD68⁺ cells were significantly higher in the core region than in the peripheral region ($P = .0002$ for CD68⁺ cells, $P = .0004$ for CD163⁺CD68⁺ cells), whereas the percentages

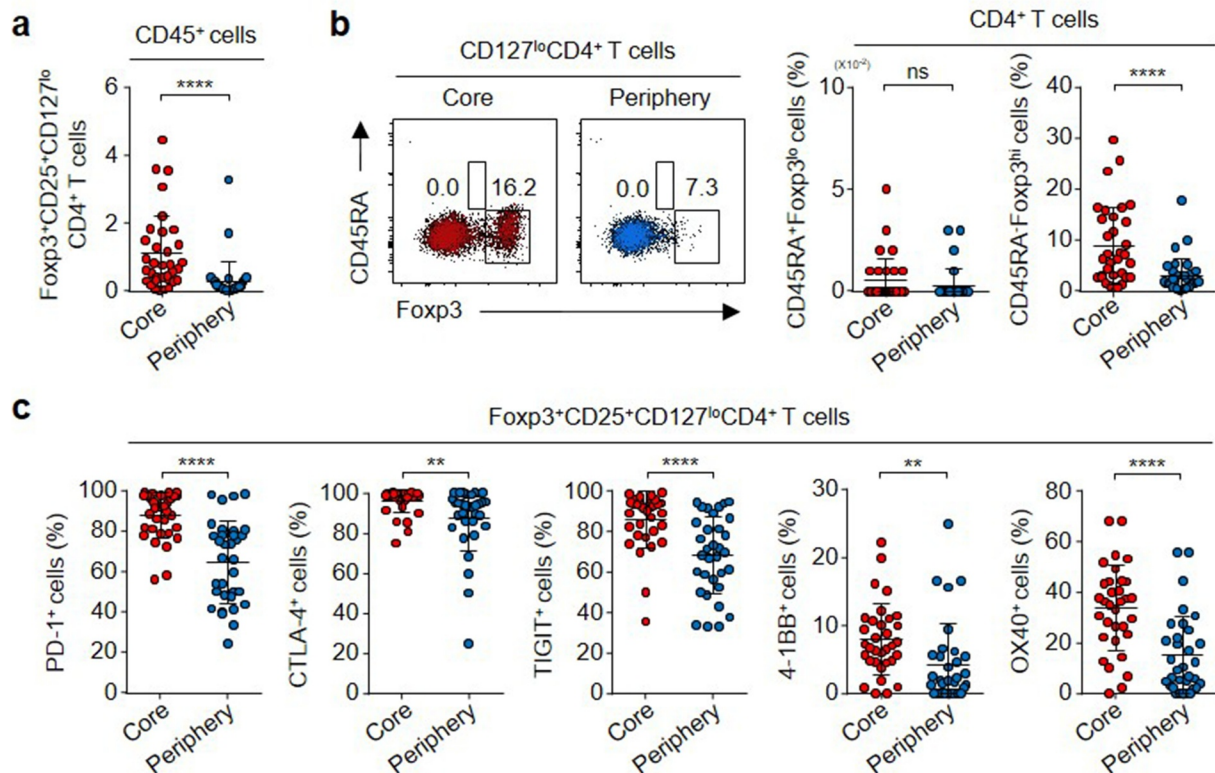


Figure 2. The infiltration and phenotypes of T_{REG} cells in the core and peripheral regions of HGG. (a) The percentages of Foxp3⁺CD25⁺CD127^{lo}CD4⁺ T cells (T_{REG} cells) among CD45⁺ cells from paired tumor core and peripheral regions ($n = 34$). **** $P < .0001$; Wilcoxon matched-pairs signed rank test. (b) The expression of Foxp3 and CD45RA among CD127^{lo}CD4⁺ T cells from paired tumor core and peripheral regions shown as representative plot from a patient (no. 12). The percentages of CD45RA⁺Foxp3^{lo} cells (naïve T_{REG} cells) and CD45RA⁻Foxp3^{hi} cells (activated T_{REG} cells) among CD4⁺ T cells from paired tumor core and peripheral regions ($n = 33$). ns, not significant; **** $P < .0001$; Wilcoxon matched-pairs signed rank test. (c) The percentages of PD-1⁺, CTLA-4⁺, TIGIT⁺, 4-1BB⁺, and OX40⁺ cells among T_{REG} cells from paired tumor core and peripheral regions ($n = 33$). ** $P < .01$; **** $P < .0001$; Wilcoxon matched-pairs signed rank test. All results were presented means \pm SD (standard deviation).

of CD163⁺ cells were not different ($P = .1349$; Figure 3b, Figure S11b). The absolute numbers of M2 monocytes, TAMs, and M2 TAMs were significantly higher in the core region than in the peripheral region (Figure S12). Taken together, the results indicate that the core region of HGG has a more immunosuppressive environment both quantitatively and qualitatively than the peripheral region.

The hypoxia signature is enriched in the core region

To determine why the core region has more severely exhausted CD8⁺ T cells and more immunosuppressive cells, we examined the transcriptomic characteristics of the core and peripheral regions in grade 4 tumors (18 pairs) using RNA-seq analysis (Figure 4a). To identify significant biological features of differentially expressed genes (DEGs), we performed gene set enrichment analysis using hallmark gene sets from MsigDB. Hypoxia, angiogenesis, and TGF- β signaling-related gene signatures were significantly enriched in the core region compared to the peripheral region (NES = 2.163, adj $P < .001$ for Hypoxia, NES = 2.35, adj $P < .001$ for Angiogenesis, NES = 1.507, adj $P = .031$ for TGF- β signaling) (Figure 4b). Next, we focused on DEGs related to the hypoxia biological process and found higher transcript levels of hypoxia-related genes in the core region (Figure 4c). To determine the significance of this biological feature in samples from the core and

peripheral regions, we performed gene set variation analysis (GSVA) using gene sets for hypoxia (hallmark), the cellular response to VEGF stimulus (Gene Ontology; GO:0035924), and the response to TGF- β (GO:0071559). We observed that the enrichment scores were significantly higher in the core regions than in the peripheral regions ($P < .0001$ for Hypoxia, $P = .0004$ for Cellular response to VEGF stimulus, $P = .0001$ for Response to TGF- β) (Figure 4d). We also found that the hypoxia score significantly correlated with transcript levels of *VEGFA* or *TGFB1* in the core region ($R = 0.83$, $P < .0001$ for *VEGFA*, $R = 0.63$, $P = .001$ for *TGFB1*) but not in the peripheral region ($R = 0.30$, $P = .22$ for *VEGFA*, $R = -0.01$, $P = .93$ for *TGFB1*) (Figure 4e). Thus, the core region of HGG is characterized by a hypoxic signature that is associated with angiogenic features and TGF- β -related features.

Immune cell phenotypes correlate with the hypoxia signature in the core region

Analyzing whether transcriptomic signatures in the core and peripheral regions are associated with the frequencies of terminally exhausted CD8⁺ T cells and immunosuppressive cells, we found that hypoxia score significantly correlated with the relative frequencies of PD-1⁺CTLA-4⁺CD8⁺ T cells ($R = 0.54$, $P = .02$), Eomes^{hi}T-bet^{lo}CD8⁺ T cells ($R = 0.49$, $P = .03$), T_{REG} cells ($R = 0.48$, $P = .04$), and M2 TAMs ($R = 0.57$, $P = .01$) in the

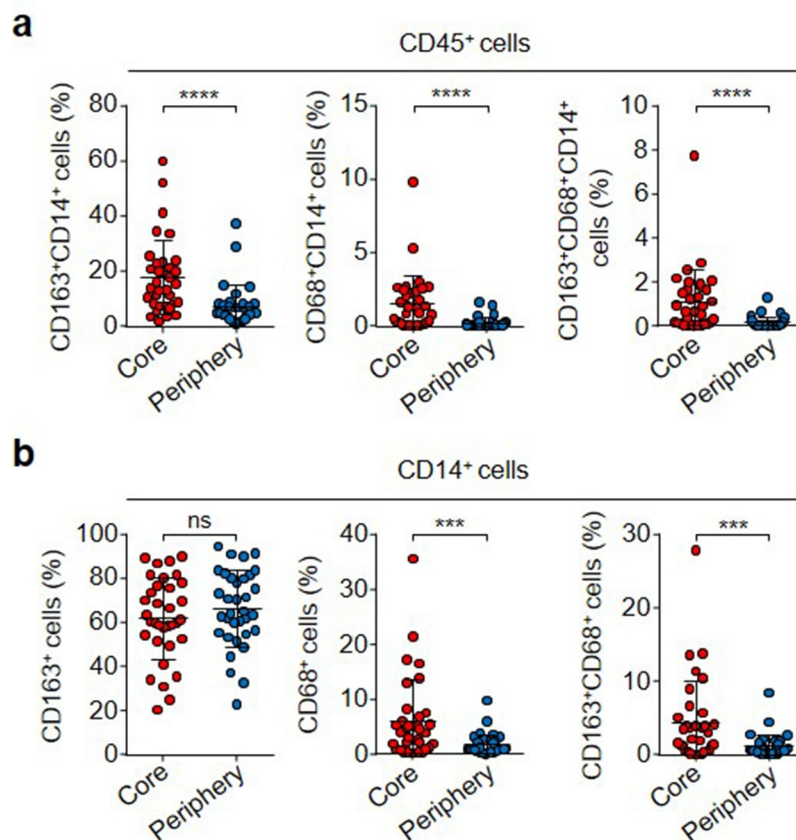


Figure 3. The infiltration and phenotypes of monocytes/macrophages in the core and peripheral regions of HGG. (a) The percentages of CD163⁺CD14⁺ cells (M2 monocytes), CD68⁺CD14⁺ cells (TAMs), and CD163⁺CD68⁺CD14⁺ cells (M2 TAMs) among CD45⁺ cells from paired tumor core and peripheral regions ($n = 34$). **** $P < .0001$; Wilcoxon matched-pairs signed rank test. (b) The percentages of CD163⁺ cells, CD68⁺ cells, and CD163⁺CD68⁺ cells among CD14⁺ cells from paired tumor core and peripheral regions ($n = 34$). ns, not significant; *** $P < .001$ using Wilcoxon matched-pairs signed rank test.

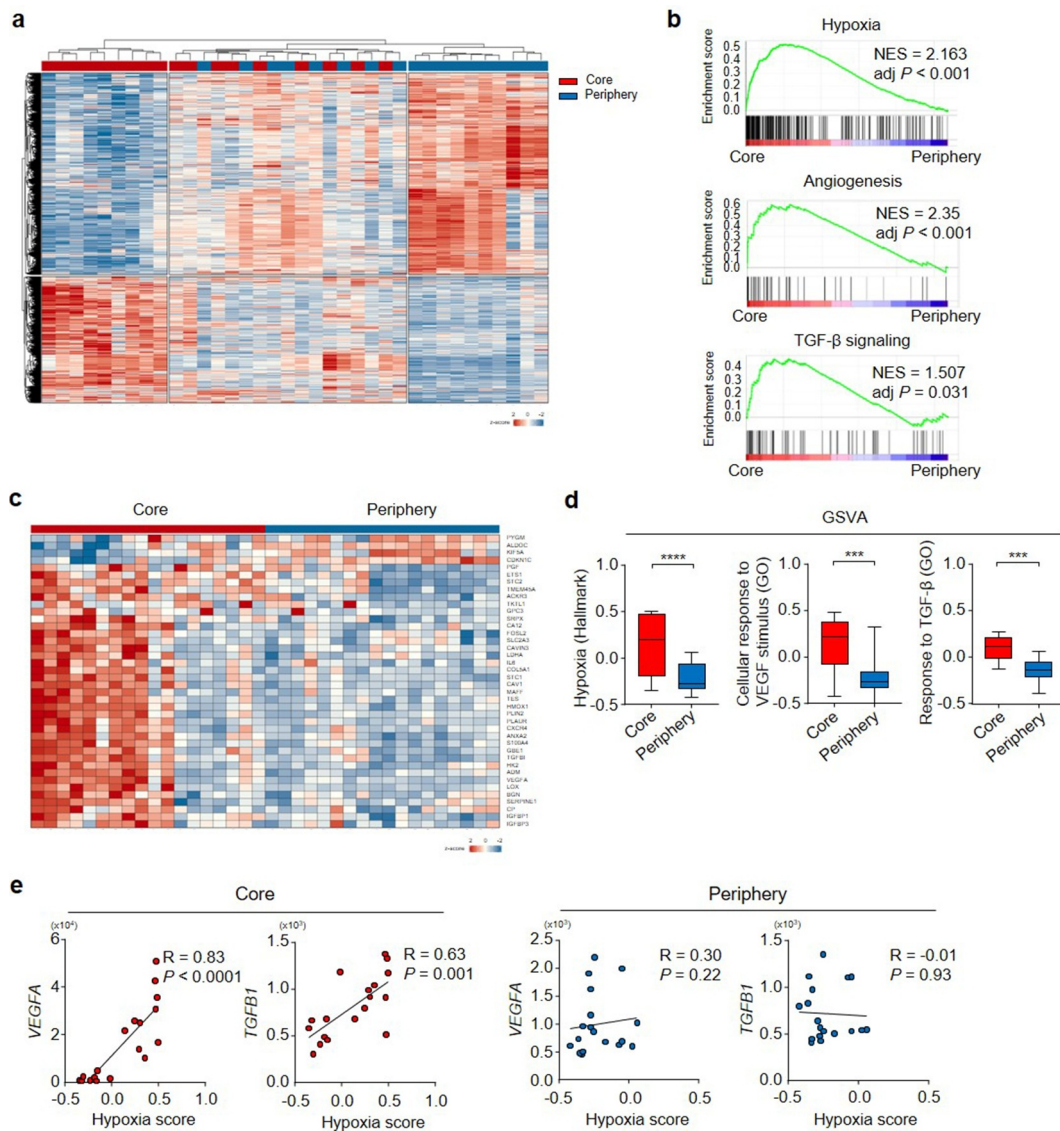


Figure 4. Distinct transcriptomic profiles in the core and peripheral regions of HGG. Bulk RNA-seq was performed with paired tumor core and peripheral tissues ($n = 18$). (a) Heat map showing the gene expression profiles. (b) Gene set enrichment analysis of differentially expressed genes (DEGs) between the tumor core and peripheral tissues using the hallmark gene sets in MSigDB. Normalized enrichment scores (NESs) and adjusted p values are presented. (c) Heat map of DEGs in the hypoxia gene set. (d) GSEA using the gene sets for Hypoxia (hallmark), Cellular response to VEGF stimulus (GO), and Response to TGF- β (GO). *** $P < .001$; **** $P < .0001$; Wilcoxon matched-pairs signed rank test. Results were presented means \pm SD (standard deviation). (e) Correlation between the hypoxia GSEA score and the normalized counts of *VEGFA* or *TGFB1* in the tumor core and peripheral tissues, respectively. Significance was assessed by Spearman correlation.

core region (Figure 5a, Figure S13a). Transcript levels of *VEGFA* significantly correlated with the relative frequencies of PD-1⁺CTLA-4⁺CD8⁺ T cells ($R = 0.50$, $P = .03$) and Eomes^{hi}T-bet^{lo}CD8⁺ T cells ($R = 0.50$, $P = .03$), and M2 TAMs ($R = 0.52$, $P = .02$), but not with the frequency of T_{REG} cells ($R = 0.33$, $P = .17$; Figure 5a, Figure S13b). These correlations were not observed when transcript levels of *TGFB1* were analyzed with the immune cell parameters, except a significant correlation between *TGFB1* and M2 TAMs ($R = 0.66$, $P = .002$; Figure 5a, Figure S13c). However, we found no association between transcriptomic signatures and the frequencies of immune cells in the peripheral region (Figure 5b, Figure S14). These data suggest that increased frequencies of terminally exhausted CD8⁺ T cells and immunosuppressive cells in the core region may be attributed to the hypoxic microenvironment.

Hypoxic conditions increase CD8⁺ T-cell exhaustion and immunosuppressive cells

To investigate whether hypoxia induces terminal exhaustion of CD8⁺ T cells and increases immunosuppressive cells, we cultured tumor-infiltrating immune cells from the peripheral region under normoxic (21% O₂) or hypoxic (1% O₂) conditions (Figure 6a). We found that hypoxia significantly increased the frequency of PD-1⁺CTLA-4⁺ cells ($P = .0156$; Figure 6b, Figure S15a) and Eomes^{hi}T-bet^{lo} cells ($P = .0156$; Figure 6c, Figure S15b) among CD8⁺ T cells. When anti-CD3-induced T-cell proliferation was assessed by CellTrace Violet (CTV) dilution assays, hypoxia significantly decreased the cellular proliferation of CD8⁺ T cells ($P = .0313$; Figure 6d, Figure S15c). In particular, hypoxia significantly increased the frequency of CTLA-4⁺ cells among T_{REG} cells ($P = .0313$; Figure 6e, Figure

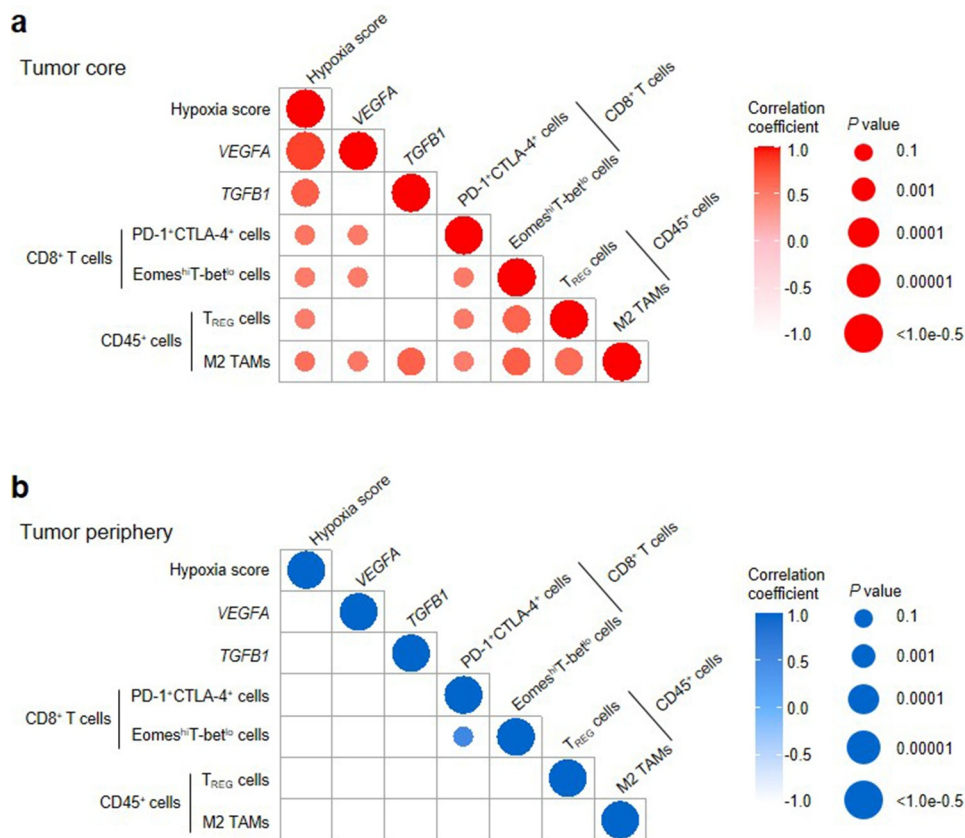


Figure 5. Correlation between the hypoxia signature and frequency of exhausted/immunosuppressive cells in the core and peripheral regions of HGG. Spearman's correlation plots for the hypoxia GSEA score, normalized counts of *VEGFA* and *TGFβ1*, and the percentages of PD-1⁺CTLA-4⁺ cells among CD8⁺ T cells, Eomes^{hi}T-bet^{lo} cells among CD8⁺ T cells, T_{REG} cells among CD45⁺ cells, and M2 TAMs among CD45⁺ cells from the core (a) and peripheral region (b) of HGG (n = 18). Correlations with $P < .05$ are considered significant and displayed as the circle. The color intensity and size of the circle represent correlation coefficient and P value, respectively.

S15d). Moreover, hypoxia significantly increased the frequency of M2 CD163⁺ cells among CD14⁺ cells ($P = .0156$; Figure 6f, Figure S15e). However, the intermediate oxygen concentration (10% O₂) did not induce the immunophenotypes observed under hypoxic conditions (Figure S16).

Investigating the effects of hypoxia on the phenotype of CD11c⁺ cells, we found that hypoxia significantly decreased the expression of CD80, CD86, and MHC-II ($P = .0156$ for CD80, $P = .0156$ for CD86, $P = .0156$ for MHC-II; Figure S17). Thus, hypoxia induces immune cell characteristics that were observed in the core region of HGG.

The frequency of PD-1⁺CTLA-4⁺CD8⁺ T cells is associated with patient survival

Finally, we analyzed whether the frequencies of exhausted CD8⁺ T cells and immunosuppressive cells are associated with the survival of patients with HGG. In survival analyses, the frequency of PD-1⁺CTLA-4⁺ cells among CD8⁺ T cells and M2 TAMs among CD45⁺ cells in the core region, but not in the peripheral region, was significantly associated with patient survival (cutoff value = 2.98%, $P = .0044$ for the core, $P = .89$ for the periphery for PD-1⁺CTLA-4⁺ cells; Figure 7a, cutoff value = 0.071%, $P = .02$ for the core, $P = .63$ for the periphery for M2 TAMs; Figure 7b). However, the frequency of Eomes^{hi}T-bet^{lo} cells

among CD8⁺ T cells was not associated with patient survival (cutoff value = 38.5%, $P = .42$ for the core, $P = .40$ for the periphery; Figure 7c). In addition, the frequencies of T_{REG} cells among CD45⁺ cells were not significantly associated with patient survival (cutoff value = 0.28%, $P = .95$ for the core, $P = .99$ for the periphery; Figure 7d). In multivariate analysis for patient survival considering age, WHO grade, KPS, IDH mutation, ATRX mutation, TERT promoter mutation, and MGMT promoter methylation, statistical significance of the frequency of PD-1⁺CTLA-4⁺ cells in the core region was preserved, but that of the frequency of M2 TAMs in the core region was not (Figure S18). Taken together, the results indicate that the increased frequency of PD-1⁺CTLA-4⁺CD8⁺ T cells under hypoxic conditions in the core region is a significant immune parameter related to the prognosis of patients with HGG.

Discussion

HGG is an aggressive tumor of the CNS with a very poor prognosis despite current standard treatment.³ Research has revealed heterogeneity of the tumor niche, which is composed of tumor cells and various immune cells, and the complexity of their interaction in the TIME of HGG.^{6,7} The specialized, complex TIME is a major clinical hurdle for devising effective

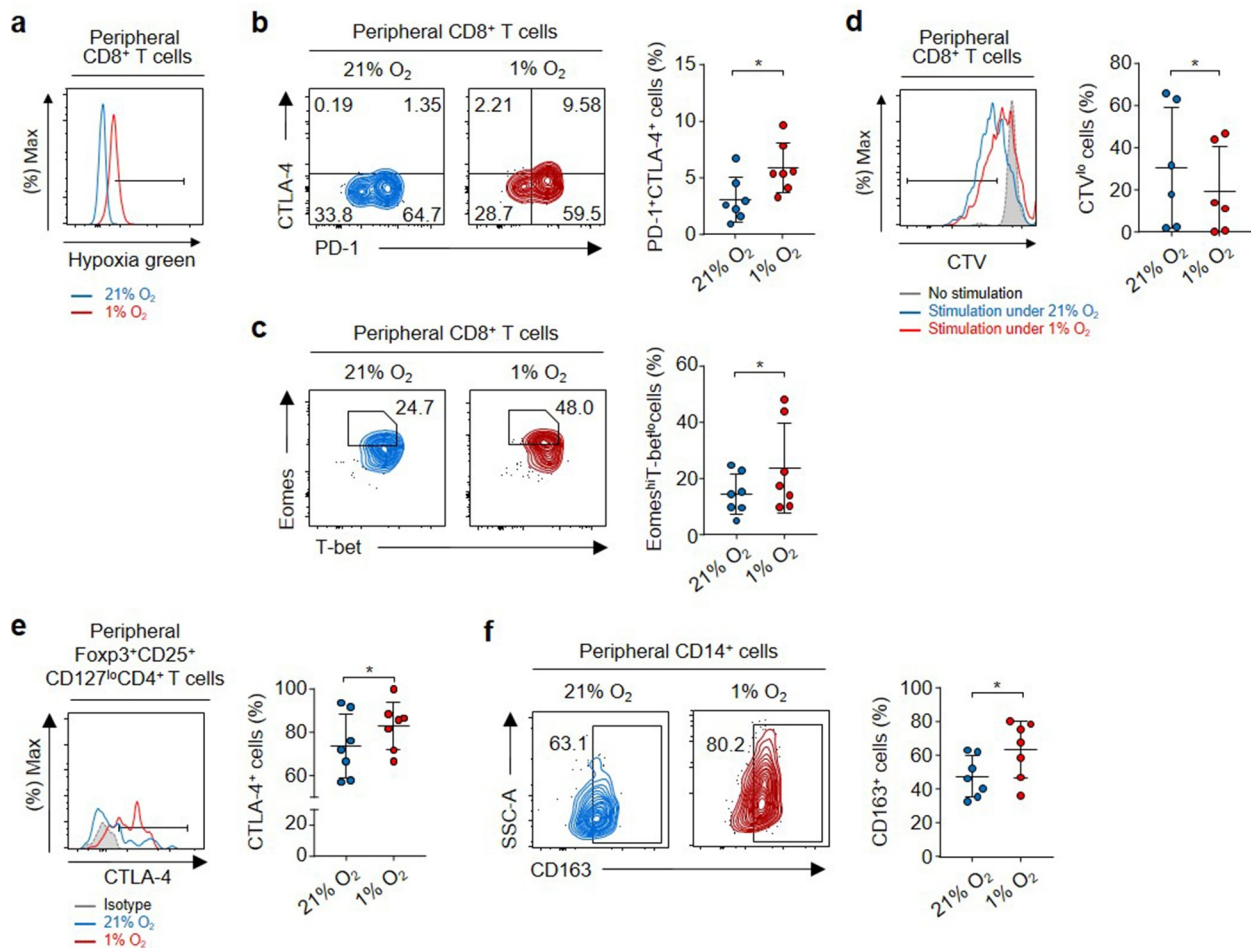


Figure 6. Effects of hypoxic conditions on immune cells in HGG. Cryopreserved cells from the peripheral regions of HGG were thawed, suspended in medium, and used for *in vitro* culture assays. (a) Cells were incubated in the presence of 0.5 μM Image-iT Green Hypoxia Reagent for 6 hours under 21% or 1% oxygen. The fluorescence intensity among CD8^+ T cells was analyzed by flow cytometry. A representative histogram is shown. (b-c) The percentages of $\text{PD-1}^+\text{CTLA-4}^+$ cells (b; $n = 7$) and $\text{Eomes}^{\text{hi}}\text{T-bet}^{\text{lo}}$ cells (c; $n = 7$) among CD8^+ T cells were analyzed by flow cytometry after culturing for 72 hours under 21% or 1% oxygen. * $P < .05$; Wilcoxon matched-pairs signed rank test. (d) CTV-labeled CD8^+ T cells were stimulated with plate-bound anti-CD3 (1 ng/ml) for 96 hours under 21% or 1% oxygen. The proliferation of CD8^+ T cells was analyzed by CTV dilution ($n = 6$). * $P < .05$; Wilcoxon matched-pairs signed rank test. (e-f) The percentages of CTLA-4^+ cells among T_{REG} cells (e; $n = 7$) and CD163^+ cells among CD14^+ cells (f; $n = 7$) were analyzed by flow cytometry after culturing for 72 hours under 21% or 1% oxygen. * $P < .05$; Wilcoxon matched-pairs signed rank test. All results were presented means \pm SD (standard deviation).

therapeutic strategies for HGG patients. Therefore, a comprehensive understanding of the TIME in HGG has been needed.

In the present study, we demonstrated distinct spatial characteristics of the HGG TIME and that the core region-enriched characteristics of tumor-infiltrating immune cells are related to microenvironment features, such as hypoxic conditions. This led to a comprehensive perspective of the HGG TIME, which may be an important consideration for the clinical approach.

Although the core and peripheral regions were not analyzed separately, several previous studies have reported exhausted and immunosuppressive phenotypes of HGG-infiltrating immune cells.^{20–22,30–34} For example, CD8^+ T cells are exhausted with attenuated effector functions in HGG^{20–22} and T_{REG} cells increased.^{30–32} In addition, M2 TAMs, which produce immunosuppressive molecules, such as arginase, IL-10, and TGF- β , accumulate in HGG.^{33,34} However, these studies have not considered immune cell heterogeneity between the tumor core and peripheral regions of HGG. In the current study, we found that tumor core-infiltrating CD8^+ T cells exhibit more severely exhausted phenotypes, as evidenced by the increased frequency of $\text{PD-1}^+\text{CTLA-4}^+$ cells and $\text{Eomes}^{\text{hi}}\text{T-bet}^{\text{lo}}$ cells.

In addition, there were more activated T_{REG} cells with higher expression of CTLA-4, an immunosuppressive molecule, and M2 TAMs in the core region. From these data, we concluded that different immune cells accumulate in the core and peripheral regions, which may contribute to the distinct features of the TIME in HGG.

In addition to the distinct distribution of immune cells in the tumor core and peripheral regions, we found an enhanced hypoxia signature in the core region. Hypoxia is one of the major biological features in the progression of brain tumors,^{53,54} particularly in the core region of HGG.^{41,42} In the current study, we demonstrated positive correlations between the hypoxia signature and the enrichment of severely exhausted CD8^+ T cells, as well as M2 TAMs and T_{REG} cells, suggesting a role of hypoxia in the origin of the immunosuppressive TIME. We directly showed that hypoxic conditions increase the number of severely exhausted CD8^+ T cells and immunosuppressive cells. Previous murine studies reported that exposure to hypoxic conditions results in enhanced expression of inhibitory immune checkpoints^{55,56} or

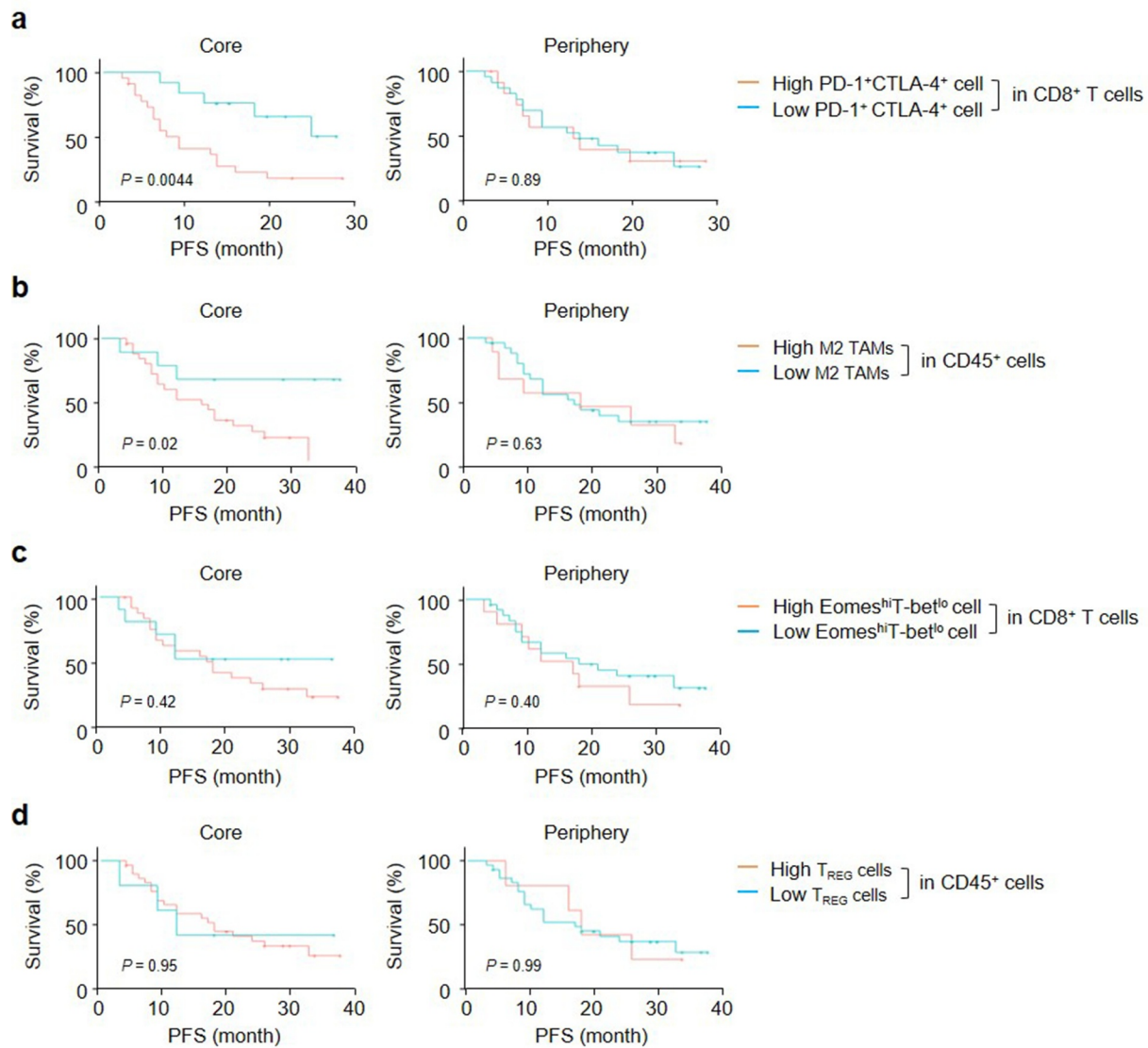


Figure 7. Relationship between immune infiltrates in tumor regions and survival of HGG patients. HGG patients were sub-grouped by the median percentages of respective subsets of immune cells from the tumor core and peripheral regions of HGG, as 'High subset' and 'Low subset'. Kaplan-Meier plots of progression-free survival (PFS) probability according to the enrichment of PD-1⁺CTLA-4⁺ cells among CD8⁺ T cells (**a**; n = 34), M2 TAMs among CD45⁺ cells (**b**; n = 34), Eomes^{hi}T-bet^{lo} cells among CD8⁺ T cells (**c**; n = 34), and T_{REG} cells among CD45⁺ cells (**d**; n = 34) from the tumor core (left) and peripheral regions (right). Significance was assessed by the log-rank test.

polarization into the anti-inflammatory M2 subset,⁵⁷ corroborating our data. Regarding the effect of hypoxia on T_{REG} cells, conflicting results have been reported.^{58,59} In the current study, we showed that hypoxia directly increased the frequency of CTLA-4⁺ T_{REG} cells. Given that CTLA-4 is one of the main immunosuppressive mechanisms of T_{REG} cells, this increase in CTLA-4⁺ T_{REG} cells indicates that the immunosuppressive functions of T_{REG} cells are enhanced. Therefore, we suggest a relationship between the hypoxic condition and immune cell changes in the HGG core TIME.

We categorized patients into high and low groups based on the relative frequency of specific immune cells infiltrating the tumor core and peripheral regions. As a result, the frequency of PD-1⁺CTLA-4⁺CD8⁺ T cells in the core region was associated with patient survival. Previously, the density

of tumor-infiltrating immune cells was reported to be associated with clinical outcome in many different tumor types.³⁹ In HGG, a high density of CD8⁺ T cells has been reported to correlate with better overall survival⁶⁰ or poor prognosis.⁶¹ The infiltration of T_{REG} cells correlated with decreased survival^{31,32} or was not associated with survival prognosis.⁶² However, previous studies did not consider differences between the core and peripheral regions of HGG. Understanding immune cell biology in different tumor regions and the underlying mechanisms will be pivotal to predicting patient prognosis and further developing therapeutic strategies that allow the TIME to be altered to more immune-favorable conditions. In this regard, the hypoxic condition in the core region needs to be modulated. Given that hypoxia directly increases CD8⁺ T-cell

exhaustion and immunosuppressive cells, correction of hypoxia will increase anti-tumor immune responses and enhance the therapeutic effects of tumor immunotherapy.

In conclusion, we investigated the distinct distribution of tumor-infiltrating immune cells and their immunophenotypes, as well as the biological signatures shaping the tumor core and peripheral microenvironments in HGG. We found that severely exhausted CD8⁺ T cells, immunosuppressive T_{REG} cells, and M2 TAMs are enriched in the core compared to the peripheral region. We also found that the hypoxia signature was enhanced in the core region and significantly related to the distribution of severely exhausted or immunosuppressive immune cells. We demonstrated that hypoxia directly increases the number of severely exhausted CD8⁺ T cells and immunosuppressive cells and confirmed the association between differences in the distribution of tumor-infiltrating immune cells and patient survival. In the future, we need to better understand the spatially heterogeneous TIME in HGG in order to develop novel immunotherapy for the treatment of patients with HGG.

Disclosure statement

The authors declare no potential conflicts of interest.

Funding

This work was supported by the National Research Foundation grants (NRF-2018M3A9D3079498 to ECS) and by a grant of the Korea Health Technology R&D Project through the Korea Health Industry Development Institute (KHIDI) funded by the Ministry of Health & Welfare, Republic of Korea (HI21C0239 to CKP).

ORCID

Eui-Cheol Shin  <http://orcid.org/0000-0002-6308-9503>

Authors' contributions

ARK and SJC: Conceptualization, Formal analysis, Investigation, Visualization, Validation, Writing-original draft. JP, MK, TC, HJY, SK, HK, KMK, and CKP: Methodology, Investigation. HK and KMK: Formal analysis, Visualization, Validation. SHP, CKP, and ECS: Supervision. CKP and ECS: Conceptualization, Writing-review & editing.

References

- Louis DN, Perry A, Reifenberger G, Von Deimling A, Figarella-Branger D, Cavenee WK, Ohgaki H, Wiestler OD, Kleihues P, Ellison DW, et al. The 2016 World Health Organization classification of tumors of the central nervous system: a summary. *Acta Neuropathol.* 2016;131(6):803–820. doi:10.1007/s00401-016-1545-1.
- Ostrom QT, Patil N, Cioffi G, Waite K, Kruchko C, Barnholtz-Sloan JS. CBTRUS statistical report: primary brain and other central nervous system tumors diagnosed in the United States in 2013-2017. *Neuro Oncol.* 2020;22(12 Suppl 2):iv1–iv96. doi:10.1093/neuonc/noaa200.
- Weller M, Wick W, Aldape K, Brada M, Berger M, Pfister SM, Nishikawa R, Rosenthal M, Wen PY, Stupp R, et al. Glioma. *Nat Rev Dis Primers.* 2015;1(1):15017. doi:10.1038/nrdp.2015.17.
- Louveau A, Smirnov I, Keyes TJ, Eccles JD, Rouhani SJ, Peske JD, Derecki NC, Castle D, Mandell JW, Lee KS, et al. Structural and functional features of central nervous system lymphatic vessels. *Nature.* 2015;523(7560):337–341. doi:10.1038/nature14432.
- Ratnam NM, Gilbert MR, Giles AJ. Immunotherapy in CNS cancers: the role of immune cell trafficking. *Neuro Oncol.* 2019;21(1):37–46. doi:10.1093/neuonc/nyy084.
- Quail DF, Joyce JA. The microenvironmental landscape of brain tumors. *Cancer Cell.* 2017;31(3):326–341. doi:10.1016/j.ccell.2017.02.009.
- Pombo Antunes AR, Scheyltjens I, Duerinck J, Neyns B, Movahedi K, Van Ginderachter JA. Understanding the glioblastoma immune microenvironment as basis for the development of new immunotherapeutic strategies. *Elife.* 2020;9. doi:10.7554/eLife.52176.
- Hashimoto M, Kamphorst AO, Im SJ, Kissick HT, Pillai RN, Ramalingam SS, Araki K, Ahmed R. CD8 T cell exhaustion in chronic infection and cancer: opportunities for interventions. *Annu Rev Med.* 2018;69(1):301–318. doi:10.1146/annurev-med-012017-043208.
- Wherry EJ, Kurachi M. Molecular and cellular insights into T cell exhaustion. *Nat Rev Immunol.* 2015;15(8):486–499. doi:10.1038/nri3862.
- Thommen DS, Koelzer VH, Herzig P, Roller A, Trefny M, Dimeloe S, Kiialainen A, Hanhart J, Schill C, Hess C, et al. A transcriptionally and functionally distinct PD-1(+) CD8(+) T cell pool with predictive potential in non-small-cell lung cancer treated with PD-1 blockade. *Nat Med.* 2018;24(7):994–1004. doi:10.1038/s41591-018-0057-z.
- Kim HD, Song GW, Park S, Jung MK, Kim MH, Kang HJ, Yoo C, Yi K, Kim KH, Eo S, et al. Association between expression level of PD1 by tumor-infiltrating CD8(+) T cells and features of hepatocellular carcinoma. *Gastroenterology.* 2018;155(6):1936–50 e17. doi:10.1053/j.gastro.2018.08.030.
- Baitsch L, Baumgaertner P, Devevre E, Raghav SK, Legat A, Barba L, Wieckowski S, Bouzourene H, Deplancke B, Romero P, et al. Exhaustion of tumor-specific CD8(+) T cells in metastases from melanoma patients. *J Clin Invest.* 2011;121(6):2350–2360. doi:10.1172/JCI46102.
- Kwon M, Kim CG, Lee H, Cho H, Kim Y, Lee EC, Choi SJ, Park J, Seo I-H, Bogen B, et al. PD-1 blockade reinvigorates bone marrow CD8(+)T cells from patients with multiple myeloma in the presence of TGFbeta inhibitors. *Clin Cancer Res.* 2020;26(7):1644–1655. doi:10.1158/1078-0432.CCR-19-0267.
- Yamamoto R, Nishikori M, Kitawaki T, Sakai T, Hishizawa M, Tashima M, Kondo T, Ohmori K, Kurata M, Hayashi T, et al. PD-1-PD-1 ligand interaction contributes to immunosuppressive microenvironment of Hodgkin lymphoma. *Blood.* 2008;111(6):3220–3224. doi:10.1182/blood-2007-05-085159.
- Paley MA, Kroy DC, Odorizzi PM, Johnnidis JB, Dolfi DV, Barnett BE, Bikoff EK, Robertson EJ, Lauer GM, Reiner SL, et al. Progenitor and terminal subsets of CD8+ T cells cooperate to contain chronic viral infection. *Science.* 2012;338(6111):1220–1225. doi:10.1126/science.1229620.
- Utzschneider DT, Charmoy M, Chennupati V, Pousse L, Ferreira DP, Calderon-Copete S, Danilo M, Alfei F, Hofmann M, Wieland D, et al. T cell factor 1-expressing memory-like CD8(+) T cells sustain the immune response to chronic viral infections. *Immunity.* 2016;45(2):415–427. doi:10.1016/j.immuni.2016.07.021.
- Jansen CS, Prokhnevskaya N, Master VA, Sanda MG, Carlisle JW, Bilen MA, Cardenas M, Wilkinson S, Lake R, Sowalsky AG, et al. An intra-tumoral niche maintains and differentiates stem-like CD8 T cells. *Nature.* 2019;576(7787):465–470. doi:10.1038/s41586-019-1836-5.
- Alfei F, Kanev K, Hofmann M, Wu M, Ghoneim HE, Roelli P, Utzschneider DT, Von Hoesslin M, Cullen JG, Fan Y, et al. TOX reinforces the phenotype and longevity of exhausted T cells in chronic viral infection. *Nature.* 2019;571(7764):265–269. doi:10.1038/s41586-019-1326-9.
- Khan O, Giles JR, McDonald S, Manne S, Ngo SF, Patel KP, Werner MT, Huang AC, Alexander KA, Wu JE, et al. TOX transcriptionally and epigenetically programs CD8(+) T cell exhaustion. *Nature.* 2019;571(7764):211–218. doi:10.1038/s41586-019-1325-x.

20. Mohme M, Schliifke S, Maire CL, Runger A, Glau L, Mende KC, Matschke J, Gehbauer C, Akyüz N, Zapf S, et al. Immunophenotyping of newly diagnosed and recurrent glioblastoma defines distinct immune exhaustion profiles in peripheral and tumor-infiltrating lymphocytes. *Clin Cancer Res.* 2018;24(17):4187–4200. doi:10.1158/1078-0432.CCR-17-2617.
21. Woroniecka K, Chongsathidkiet P, Rhodin K, Kemeny H, Dechant C, Farber SH, Elsamadicy AA, Cui X, Koyama S, Jackson C, et al. T-cell exhaustion signatures vary with tumor type and are severe in glioblastoma. *Clin Cancer Res.* 2018;24(17):4175–4186. doi:10.1158/1078-0432.CCR-17-1846.
22. Park J, Kwon M, Kim KH, Kim TS, Hong SH, Kim CG, Kang S-G, Moon JH, Kim EH, Park S-H, et al. Immune checkpoint inhibitor-induced reinvigoration of tumor-infiltrating CD8(+) T cells is determined by their differentiation status in glioblastoma. *Clin Cancer Res.* 2019;25(8):2549–2559. doi:10.1158/1078-0432.CCR-18-2564.
23. Plitas G, Rudensky AY. Regulatory T cells in cancer. *Ann Rev Cancer Biol.* 2020;4(1):459–477. doi:10.1146/annurev-cancerbio-030419-033428.
24. De Simone M, Arrigoni A, Rossetti G, Gruarin P, Ranzani V, Politano C, Bonnal RP, Provasi E, Sarnicola M, Panzeri I, et al. Transcriptional landscape of human tissue lymphocytes unveils uniqueness of tumor-infiltrating T regulatory cells. *Immunity.* 2016;45(5):1135–1147. doi:10.1016/j.immuni.2016.10.021.
25. Azizi E, Carr AJ, Plitas G, Cornish AE, Konopacki C, Prabhakaran S, Nainys J, Wu K, Kiseliovas V, Setty M, et al. Single-cell map of diverse immune phenotypes in the breast tumor microenvironment. *Cell.* 2018;174(5):1293–308 e36. doi:10.1016/j.cell.2018.05.060.
26. Movahedi K, Laoui D, Gysemans C, Baeten M, Stange G, Van Den Bossche J, Mack M, Pipeleers D, In't Veld P, De Baetselier P, et al. Different tumor microenvironments contain functionally distinct subsets of macrophages derived from Ly6C(high) monocytes. *Cancer Res.* 2010;70(14):5728–5739. doi:10.1158/0008-5472.CAN-09-4672.
27. Ruffell B, Chang-Strachan D, Chan V, Rosenbusch A, Ho CM, Pryer N, Daniel D, Hwang E, Rugo H, Coussens L, et al. Macrophage IL-10 blocks CD8+ T cell-dependent responses to chemotherapy by suppressing IL-12 expression in intratumoral dendritic cells. *Cancer Cell.* 2014;26(5):623–637. doi:10.1016/j.ccr.2014.09.006.
28. Mantovani A, Sozzani S, Locati M, Allavena P, Sica A. Macrophage polarization: tumor-associated macrophages as a paradigm for polarized M2 mononuclear phagocytes. *Trends Immunol.* 2002;23(11):549–555. doi:10.1016/S1471-4906(02)02302-5.
29. Benner B, Scarberry L, Suarez-Kelly LP, Duggan MC, Campbell AR, Smith E, Lapurga G, Jiang K, Butchar JP, Tridandapani S, et al. Generation of monocyte-derived tumor-associated macrophages using tumor-conditioned media provides a novel method to study tumor-associated macrophages in vitro. *J Immunother Cancer.* 2019;7(1):140. doi:10.1186/s40425-019-0622-0.
30. El Andaloussi A, Lesniak MS. An increase in CD4+CD25+FOXP3+ regulatory T cells in tumor-infiltrating lymphocytes of human glioblastoma multiforme. *Neuro Oncol.* 2006;8(3):234–243. doi:10.1215/15228517-2006-006.
31. Yue Q, Zhang X, Ye HX, Wang Y, Du ZG, Yao Y, Mao Y. The prognostic value of Foxp3+ tumor-infiltrating lymphocytes in patients with glioblastoma. *J Neurooncol.* 2014;116(2):251–259. doi:10.1007/s11060-013-1314-0.
32. Sayour EJ, McLendon P, McLendon R, De Leon G, Reynolds R, Kresak J, Sampson JH, Mitchell DA. Increased proportion of FoxP3+ regulatory T cells in tumor infiltrating lymphocytes is associated with tumor recurrence and reduced survival in patients with glioblastoma. *Cancer Immunol Immunother.* 2015;64(4):419–427. doi:10.1007/s00262-014-1651-7.
33. Hussain SF, Yang D, Suki D, Aldape K, Grimm E, Heimberger AB. The role of human glioma-infiltrating microglia/macrophages in mediating antitumor immune responses. *Neuro Oncol.* 2006;8(3):261–279. doi:10.1215/15228517-2006-008.
34. Hambardzumyan D, Gutmann DH, Kettenmann H. The role of microglia and macrophages in glioma maintenance and progression. *Nat Neurosci.* 2016;19(1):20–27. doi:10.1038/nn.4185.
35. Yuan Y. Spatial heterogeneity in the tumor microenvironment. *Cold Spring Harb Perspect Med.* 2016;6(8):a026583. doi:10.1101/cshperspect.a026583.
36. Estrella V, Chen T, Lloyd M, Wojtkowiak J, Cornnell HH, Ibrahim-Hashim A, Bailey K, Balagurunathan Y, Rothberg JM, Sloane BF, et al. Acidity generated by the tumor microenvironment drives local invasion. *Cancer Res.* 2013;73(5):1524–1535. doi:10.1158/0008-5472.CAN-12-2796.
37. Puram SV, Tirosch I, Parikh AS, Patel AP, Yizhak K, Gillespie S, Rodman C, Luo CL, Mroz EA, Emerick KS, et al. Single-cell transcriptomic analysis of primary and metastatic tumor ecosystems in head and neck cancer. *Cell.* 2017;171(7):1611–24 e24. doi:10.1016/j.cell.2017.10.044.
38. Hasnim M, Noman MZ, Messai Y, Bordereaux D, Gros G, Baud V, Chouaib S. Cutting edge: hypoxia-induced Nanog favors the intratumoral infiltration of regulatory T cells and macrophages via direct regulation of TGF-beta1. *J Immunol.* 2013;191(12):5802–5806. doi:10.4049/jimmunol.1302140.
39. Fridman WH, Pages F, Sautes-Fridman C, Galon J. The immune contexture in human tumours: impact on clinical outcome. *Nat Rev Cancer.* 2012;12(4):298–306. doi:10.1038/nrc3245.
40. Vartanian A, Singh SK, Agnihotri S, Jalali S, Burrell K, Aldape KD, Zadeh G. GBM's multifaceted landscape: highlighting regional and microenvironmental heterogeneity. *Neuro Oncol.* 2014;16(9):1167–1175. doi:10.1093/neuonc/nou035.
41. Darmanin S, Sloan SA, Croote D, Mignardi M, Chernikova S, Samghababi P, Zhang Y, Neff N, Kowarsky M, Caneda C, et al. Single-cell RNA-seq analysis of infiltrating neoplastic cells at the migrating front of human glioblastoma. *Cell Rep.* 2017;21(5):1399–1410. doi:10.1016/j.celrep.2017.10.030.
42. Tamura R, Ohara K, Sasaki H, Morimoto Y, Kosugi K, Yoshida K, Toda M. Difference in immunosuppressive cells between peritumoral area and tumor core in glioblastoma. *World Neurosurg.* 2018;120:e601–e10. doi:10.1016/j.wneu.2018.08.133.
43. Stummer W, Pichlmeier U, Meinel T, Wiestler OD, Zanella F, Reulen HJ. Fluorescence-guided surgery with 5-aminolevulinic acid for resection of malignant glioma: a randomised controlled multicentre phase III trial. *Lancet Oncol.* 2006;7(5):392–401. doi:10.1016/S1470-2045(06)70665-9.
44. Kim S, Kim JE, Kim YH, Hwang T, Kim SK, Xu WJ, Shin J-Y, Kim J-I, Choi H, Kim HC, et al. Glutaminase 2 expression is associated with regional heterogeneity of 5-aminolevulinic acid fluorescence in glioblastoma. *Sci Rep.* 2017;7(1):12221. doi:10.1038/s41598-017-12557-3.
45. Kim AR, Choi KS, Kim M-S, Kim K-M, Kang H, Kim S, Chowdhury T, Yu HJ, Lee CE, Lee JH, et al. Absolute quantification of tumor-infiltrating immune cells in high-grade glioma identifies prognostic and radiomics values. *Cancer Immunol Immunother.* 2021;70(7):1995–2008. doi:10.1007/s00262-020-02836-w.
46. Dobin A, Davis CA, Schlesinger F, Drenkow J, Zaleski C, Jha S, Batut P, Chaisson M, Gingeras TR. STAR: ultrafast universal RNA-seq aligner. *Bioinformatics.* 2013;29(1):15–21. doi:10.1093/bioinformatics/bts635.
47. Love MI, Huber W, Anders S. Moderated estimation of fold change and dispersion for RNA-seq data with DESeq2. *Genome Biol.* 2014;15(12):550. doi:10.1186/s13059-014-0550-8.
48. Yu G, Wang LG, Han Y, He QY. clusterProfiler: an R package for comparing biological themes among gene clusters. *OMICS.* 2012;16(5):284–287. doi:10.1089/omi.2011.0118.
49. Hanzelmann S, Castelo R, Guinney J. GSEA: gene set variation analysis for microarray and RNA-seq data. *BMC Bioinform.* 2013;14:7. doi:10.1186/1471-2105-14-7.
50. Blackburn SD, Shin H, Freeman GJ, Wherry EJ. Selective expansion of a subset of exhausted CD8 T cells by aPD-L1 blockade. *Proc Natl Acad Sci.* 2008;105(39):15016–15021. doi:10.1073/pnas.0801497105.

51. Takahashi T, Tagami T, Yamazaki S, Uede T, Shimizu J, Sakaguchi N, Mak TW, Sakaguchi S. Immunologic self-tolerance maintained by CD25(+)CD4(+) regulatory T cells constitutively expressing cytotoxic T lymphocyte-associated antigen 4. *J Exp Med*. 2000;192(2):303–310. doi:10.1084/jem.192.2.303.
52. Peggs KS, Quezada SA, Chambers CA, Korman AJ, Allison JP. Blockade of CTLA-4 on both effector and regulatory T cell compartments contributes to the antitumor activity of anti-CTLA-4 antibodies. *J Exp Med*. 2009;206(8):1717–1725. doi:10.1084/jem.20082492.
53. Evans SM, Judy KD, Dunphy I, Jenkins WT, Nelson PT, Collins R, Wileyto EP, Jenkins K, Hahn SM, Stevens CW, et al. Comparative measurements of hypoxia in human brain tumors using needle electrodes and EF5 binding. *Cancer Res*. 2004;64(5):1886–1892. doi:10.1158/0008-5472.CAN-03-2424.
54. Evans SM, Judy KD, Dunphy I, Jenkins WT, Hwang WT, Nelson PT, Lustig RA, Jenkins K, Magarelli DP, Hahn SM, et al. Hypoxia is important in the biology and aggression of human glial brain tumors. *Clin Cancer Res*. 2004;10(24):8177–8184. doi:10.1158/1078-0432.CCR-04-1081.
55. Doedens AL, Phan AT, Stradner MH, Fujimoto JK, Nguyen JV, Yang E, Johnson RS, Goldrath AW. Hypoxia-inducible factors enhance the effector responses of CD8(+) T cells to persistent antigen. *Nat Immunol*. 2013;14(11):1173–1182. doi:10.1038/ni.2714.
56. Palazon A, Tyrakis PA, Macias D, Velica P, Rundqvist H, Fitzpatrick S, Vojnovic N, Phan AT, Loman N, Hedenfalk I, et al. An HIF-1 α /VEGF-A axis in cytotoxic T cells regulates tumor progression. *Cancer Cell*. 2017;32(5):669–83 e5. doi:10.1016/j.ccell.2017.10.003.
57. Leblond MM, Gerault AN, Corroyer-Dulmont A, MacKenzie ET, Petit E, Bernaudin M, Valable S, et al. Hypoxia induces macrophage polarization and re-education toward an M2 phenotype in U87 and U251 glioblastoma models. *Oncoimmunology*. 2016;5(1):e1056442. doi:10.1080/2162402X.2015.1056442.
58. Dang EV, Barbi J, Yang HY, Jinasena D, Yu H, Zheng Y, Bordman Z, Fu J, Kim Y, Yen H-R, et al. Control of T(H)17/T(reg) balance by hypoxia-inducible factor 1. *Cell*. 2011;146(5):772–784. doi:10.1016/j.cell.2011.07.033.
59. Clambey ET, McNamee EN, Westrich JA, Glover LE, Campbell EL, Jedlicka P, de Zoeten EF, Cambier JC, Stenmark KR, Colgan SP, et al. Hypoxia-inducible factor-1 alpha-dependent induction of FoxP3 drives regulatory T-cell abundance and function during inflammatory hypoxia of the mucosa. *Proc Natl Acad Sci USA*. 2012;109(41):E2784–93. doi:10.1073/pnas.1202366109.
60. Yang I, Tihan T, Han SJ, Wrensch MR, Wiencke J, Sughrue ME, Parsa AT. CD8+ T-cell infiltrate in newly diagnosed glioblastoma is associated with long-term survival. *J Clin Neurosci*. 2010;17(11):1381–1385. doi:10.1016/j.jocn.2010.03.031.
61. Marinari E, Allard M, Gustave R, Widmer V, Philippin G, Merkler D, Tsantoulis P, Dutoit V, Dietrich P-Y. Inflammation and lymphocyte infiltration are associated with shorter survival in patients with high-grade glioma. *Oncoimmunology*. 2020;9(1):1779990. doi:10.1080/2162402X.2020.1779990.
62. Heimberger AB, Abou-Ghazal M, Reina-Ortiz C, Yang DS, Sun W, Qiao W, Hiraoka N, Fuller GN. Incidence and prognostic impact of FoxP3+ regulatory T cells in human gliomas. *Clin Cancer Res*. 2008;14(16):5166–5172. doi:10.1158/1078-0432.CCR-08-0320.